SEMARAK ILMU PUBLISHING

Journal of Advanced Research in Fluid Mechanics and Thermal Sciences

Journal homepage: https://semarakilmu.com.my/journals/index.php/fluid_mechanics_thermal_sciences/index
ISSN: 2289-7879

Joint Effect of Velocity Slip and Joule Heating MHD Casson-Williamson Nanofluid Passes Through the Stretching Porous Medium

Yuvaraju Namala[1], Dyapa Hymavathi[2], Ramesh Kune[1,*], Borra Shashidar Reddy[1]

[1] Department of Mathematics, Sreenidhi Institute of Science and Technology, Hyderabad, Telangana, India
[2] Department of Mathematics, University College of Science, Mahatma Gandhi University, Nalgonda, Telangana, India

ARTICLE INFO

Article history:
Received 1 June 2024
Received in revised form 7 October 2024
Accepted 16 October 2024
Available online 30 October 2024

ABSTRACT

The objective of this study is to examine the heat and mass transport characteristics of a non-Newtonian Casson-Williamson nanofluid flow over a porous stretching sheet. The viscoelastic characteristic of a fluid is obtained by combining Casson and Williamson fluids. It is anticipated that the porous media through which the non-Newtonian fluid flows will adhere to Darcy's law. The effects of magnetic and electric fields are taken into account. The mathematical modeling of this physical problem involves a set of nonlinear partial differential equations that are mass, energy and momentum, together with corresponding boundary conditions, these PDEs are transformed into dimensionless ODE by appropriate similarity transformations and solved by R-K method. The numerical analysis is subsequently presented in a visual format to illustrate the influence of different controlling parameters on velocity, temperature, and concentration. Moreover, the analysis gives higher values of magnetic, viscous dissipation and joule heating parameters leads the temperature and Nusselt number. Conversely an increasing in mixed convection parameter result in a depreciation in the temperature. The skin-friction coefficient exhibited an upward trend with an increase in the porosity parameter. The rate of heat transfer demonstrated a rise under the Joule heating conditions. These findings are compared to other recorded results for a specific situation, then displayed graphically and analyzed in terms of engineering and industrial implications. Novelty this paper is by adding joule heating to nanofluid control over heat dissipation, thermal stability, or enhanced efficiency in heat exchange applications.

Keywords:
Casson nanofluid; Williamson nanofluid; MHD; porous medium; velocity slip and joule heating

1. Introduction

Nano fluids are considered as class of engineering fluids with base fluids are chosen as (water kerosene and Ethylene Glycol) and dispersed nano particles with size (1-100nm). Here we can choose the base fluids based on specific applications such as viscosity and temperature. Due to more applications of Nano fluids such as cooling of electronics, heat transfer systems, biomedical devices and thermal energy storage. Many researchers are made an attempt to explain the integrity of fluid dynamics in a diversity of practical applications in order to better understand its rheology. So,

* *Corresponding author.*
E-mail address: formularamesh@gmail.com

https://doi.org/10.37934/arfmts.123.1.156171

scientists and engineers focus their research on Nano fluids. The nanofluids exhibit various rheological feature witnessed more useful to the chemical engineering, biomedical sciences, pharmaceutical applications [1]. Variable fluid properties of a steady mixed convection of non-Newtonian Nano fluid contain microorganism in saturated non-Darcy porous medium investigated by Nima *et al.,* [2]. The ability of nanotechnology to connect molecular, atomic and micro structural engineering was discussed by El-Khatib *et al.,* [3,4] and Khalil *et al.,* [5]. Examined the mixed convective boundary layer flow of a non-Newtonian nanofluid in the vicinity of a vertical stretching surface by Buongiorno [6]. Impact of Second order chemical reaction on hybrid nanofluid passes through a vertical plate was studied by Kumar *et al.,* [7]. Reported a study on nanofluid flow via porous media and nanofluid flow with slip effect [8]. The study of the behavior of conducting fluids in the presence of magnetic fields is known as magnetohydrodynamics (MHD). This includes plasmas, liquid metals, and ionized gases. It describes and understands the complicated interactions between the fluid motion and the magnetic field by combining principles from fluid mechanics, electromagnetism, and plasma physics. Magnetohydrodynamics (MHD) has several applications in physics, chemistry, and engineering. MHD tackles key physical processes at multiple length scales, ranging from biological systems to astronomical phenomena such as solar flares. It also uses in heat-reducing applications such as joining procedures and electric arc welding heat reducing, as well as other technologically relevant applications such as fusion plasma magnetic confinement and interaction with projected liquid metal blankets. Investigated the impact of Magnetic field on MHD micro polar non-Newtonian by Patel *et al.,* [9].

Saeed *et al.,* [10] explores, in a porous-surfaced plate with generalized boundary conditions, an analytical solution of incompressible and magnetic Casson fluid in Darcy's medium that is dependent on temperature and concentration. The homotopic analysis method (HAM) and BVP4C (a Matlab routine) for the numerical modeling and analysis of an unsteady Carreau fluid with a magnetohydrodynamical influence over a stretching sheet explained by Qayyum *et al.,* [11].

MHD research is motivated by many applications, including magnetic resonance imaging for tumor diagnosis, the peristaltic activity of the ureter scanned by large magnetic resistive sensors, space and astrophysical plasma description, and the use of magnets to propel liquid metals from previous studies [11,12].

Numerical investigation of transient MHD current on a vertical plate accelerated exponentially with Hall current and chemical processes is explained by Megaraju *et al.,* [13]. Heat transfer in thermal engineering refers to the exchange of thermal energy in fluid flow. Through numerical models and experiments, the understanding of MHD thermosolutal convection with magnetism and flow dynamics is improved.

In recent years, non- Newtonian fluids have contributed significantly in industrial innovation. The fluids display diverse rheological properties, making them more valuable in biomedical sciences, pharmaceuticals, chemical engineering and other fields than Newtonian fluids [14]. However, the liquid's non-linear viscoelastic nature makes it difficult to stimulate and forecast industrial operations. However, in nature some of the non-Newtonian materials are not elastic from previous studies [15,16]. Casson fluid is one of the most commonly utilized viscoelastic non-Newtonian materials. The fluid substance has zero viscosity at infinite nonlinear shear rate and its yield stress does not initiate flow [17]. Based on the applicability of Casson fluids, the consequence of heat distribution on the flow of conducting Casson material across an expanding surface was investigated by Qing *et al.,* [18]. The investigation verified that the application of Newtonian heating enhances the dispersion of heat while simultaneously reducing the viscosity of non-Newtonian substances. Khan *et al.,* [19] studied Casson liquid colloidal reactions that involved both heterogeneous and homogeneous chemical species. A study of numerical data was presented, leading to the conclusion that the Casson term influenced the flow motion by increasing the viscosity. However, mixing Casson and Williamson fluid increases its industrial value. As the shear stress rate increases, the viscosity of the Williamson fluid decreases, making it a shear-thinning liquid. In order to explore the chemical species reaction of Williamson fluid in a boundary film system, the homotopy technique was utilized. Flow velocity and heat dissipation were both shown to decrease when the Williamson term was raised, as indicated by Khan *et al.,* [20]. Khan and Hamid [21] investigated the Williamson fluid mass diffusion flow heat transport over a wedge-geometry apparatus, with the numerical results recommend that raising the Williamson thermofluid term minimizes species reaction diffusion. The effects of heat transport and radiation on the Williamson reactive fluid were discussed individually in previous studies [22,23]. Convectional heat transfer and heat conductivity strength of Casson and Williamson fluids are increased when engineering colloidal nanoparticles are added to a base fluid, leading to maximum productivity of nanotechnological and industrial products. According to the numerical results, the stretching velocity term had a significant influence on fluid viscosity and thermal conduction.

Explored the impact of Thompson and non-Carreau nanofluid flow over a stretchable inclined by Shaw and team members of previous studies [24,25].

The combination of non-Newtonian Casson -Williamson models Studies demonstrate the importance of physical characteristics, which results in fluids could be called as a Casson-Williamson models explored by Humane *et al.,* [26]. A study on the mass transfer and MHD boundary layer flow of nanofluid through a nonlinear stretching plate with chemical reaction by Reddy *et al.,* [27]. An infinite vertical inclined porous plate is passed by a free convective Casson fluid flow with combined radiation absorption and chemical reaction effect by Swarnalathamma *et al.,* [28].

The use of boundary layer flow momentum and heat transfer across a stretching sheet has been utilized in several chemical engineering procedures, including metallurgical and polymer extrusion operations that require cooling a molten liquid before it is stretched into a cooling system. Yousef *et al.,* [29] examined the influence viscous dissipation on of a non-Newtonian CWN flow with a slippery linear stretching surface through porous medium. Explained the Thermal radiation and joule effect on Casson nanofluids which passes through the non-linear inclined sheet in the presence of chemical reaction [30]. Nadeem and Hussain [31] examined characteristics of non-Newtonian Williamson fluid passes through the exponential stretching sheet.

By examine the previous investigations didn't take into account the effects of slip velocity, Joule effects, and mixed convection on Casson–Williamson nanofluid. The result of current flow in a conductor producing thermal energy is called joule heating. This is demonstrated by an increase in the conductor temperature. Following the energy conservation principle, the Joule heating transforms "electrical energy" into "thermal energy. ′′The Joule heat effect become importance; researchers made a progress on this topic. Our contribution represents a significant advancement in nanofluid dynamics and heat exchange, expanding the current state of knowledge and potentially benefiting a variety of applications. These applications include the design of heat exchangers that are more efficient, cooling systems for electronic devices, and the improvement of thermal therapies in biomedical applications.

In the present study, we analyze the Casson –Williamson nanofluid stretchable flow in the presence Joint effect of velocity slip and Joule heating. The governing systems of partial equations have been transformed to set of coupled ordinary differential equations with the help of suitable similarity transformations. The reduced equations are solved numerically. The effects of different flow pertinent parameters on velocity, temperature and concentration profiles are elucidated through graphs and tables. The comparison is made with existing results for some limiting cases and is found to be in good agreement.

The novel aspect of this study is that it looks at how well chemical reactions happen when nano particles move because of Joule heating, as well as the slip velocity for a Casson-Williamson non-Newtonian nanofluid.

There is a gap in understanding how velocity slip and Joule heating interact synergistically or antagonistically in Casson-Williamson nanofluids. Most existing studies focus on one effect in isolation or assume negligible interactions. While there is research on non-Newtonian nanofluids, the specific behavior of Casson-Williamson nanofluids under slip conditions and Joule heating remains understudied. The Casson model introduces yield stress, which can significantly influence flow patterns and thermal characteristics.

2. Formulation of the Problem

The governing equations of the Casson-Williamson fluid are employed as a representation of a non-Newtonian Nanofluid. The relation between shear stress τ_{ij} and the constitutive equation which refers the Williamson model is built and used by Nadeem and Hussain [31] and is mentioned as follows.

$$\tau_{ij} = \mu\left(\frac{\partial u}{\partial y} + \frac{\Gamma}{\sqrt{2}}\left(\frac{\partial u}{\partial y}\right)^2\right) \tag{1}$$

Here Γ is the time constant and μ is viscosity of the fluid. When Γ = 0 the model represents Newtonian model. Following relationship gives the Casson fluid model.

$$\tau_{ij} = \mu\left(\left(1 + \frac{1}{\beta}\right)\frac{\partial u}{\partial y}\right) \tag{2}$$

where β is a Casson parameter the present model is characterized by [26]

$$\tau_{ij} = \mu\left(\left(1 + \frac{1}{\beta}\right)\frac{\partial u}{\partial y} + \frac{\Gamma}{\sqrt{2}}\left(\frac{\partial u}{\partial y}\right)^2\right) \tag{3}$$

Under these constraints a uniform magnetic field of strength B_0 is supposed along the Y-axis and the induced magnetic field is negligible compared to applied field. Under the effects of Joule heating, magnetic field and slip velocity on the fluid flow. Consider T and C the temperature and concentration of a nanofluid, v, u be the components of nanofluid velocity. For the flow of steady, two-dimensional laminar of Casson-Williamson model has the following governing differential equations and the physical model has shown in Figure 1.

Assumptions:

The fluid is assumed to follow the Casson-Williamson model, which considers non-Newtonian behavior with yield stress and shear-thinning characteristics. This involves assuming a relationship between shear stress and shear rate that adheres to the Casson model's principles.

The fluid is considered electrically conducting and subject to an external magnetic field. Assumptions may include a steady magnetic field and negligible induced magnetic field effects (low magnetic Reynolds number).

The stretching porous medium is often modeled as a permeable medium with constant stretching velocity. Assumptions may include Darcy's law for fluid flow through the porous medium and constant porosity.

A slip boundary condition is assumed at the stretching surface, where the fluid velocity is greater than zero. The slip parameter accounts for the slip effects between the fluid and the solid surface.

Joule heating is considered due to the presence of an electric field in the fluid. Assumptions may include steady-state electrical conductivity, uniform electric field distribution, and neglecting magnetic field effects on electrical conductivity (if applicable).

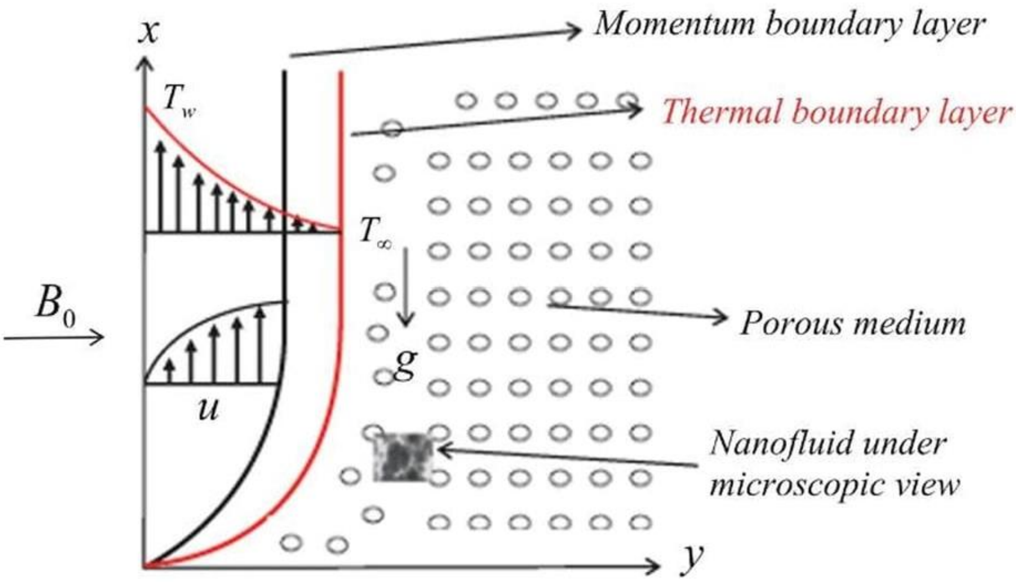

Fig. 1. Physical model of the problem

Governing Equation [29]

$$\frac{\partial u}{\partial x}+\frac{\partial v}{\partial y}=0 \tag{4}$$

$$u\frac{\partial u}{\partial x}+v\frac{\partial u}{\partial y}=\gamma\left(1+\frac{1}{\beta}\right)\frac{\partial^2 u}{\partial y^2}+\sqrt{2}\gamma\Gamma\frac{\partial u}{\partial y}\frac{\partial^2 u}{\partial y^2}-\frac{\sigma B_0^2}{\rho}u-\frac{\gamma}{k}u+g\beta'(T-T_\infty) \tag{5}$$

$$u\frac{\partial T}{\partial x}+v\frac{\partial T}{\partial y}=\frac{\kappa}{\rho C_p}\left(1+\frac{16\sigma^* T_\infty^3}{3k\kappa}\right)\frac{\partial^2 T}{\partial y^2}+\tau\left\{D_B\frac{\partial C}{\partial y}\frac{\partial T}{\partial y}+\frac{D_T}{T_\infty}\left(\frac{\partial T}{\partial y}\right)^2\right\}+\frac{\mu}{\rho C_p}\left[\left(1+\frac{1}{\beta}\right)\left(\frac{\partial u}{\partial y}\right)^2+\frac{\Gamma}{\sqrt{2}}\left(\frac{\partial u}{\partial y}\right)^3\right]+$$
$$\frac{Q_0}{\rho C_p}(T-T_\infty)+\frac{\sigma B_0^2}{\rho C_p}u^2 \tag{6}$$

Concentration Equation

$$u\frac{\partial C}{\partial x}+v\frac{\partial C}{\partial y}=D_B\frac{\partial^2 C}{\partial y^2}+\frac{D_T}{T_\infty}\frac{\partial^2 T}{\partial y^2}-k_q(C-C_\infty) \tag{7}$$

Boundary Conditions [29]

$$u=ax+\lambda_1\left[\left(1+\frac{1}{\beta}\right)\frac{\partial u}{\partial y}+\frac{\Gamma}{\sqrt{2}}\left(\frac{\partial u}{\partial y}\right)^2\right]v \text{ at} = 0, T=T_w,\; C=C_w\, at\; y=0$$
$$u\to 0, T\to T_\infty, C\to C_\infty, as\; y\to\infty \tag{8}$$

Similarity Transformations

$$\eta = y\sqrt{\frac{a}{\gamma}},\ \ u = axf'(\eta)\ ,\ \ v = -\sqrt{a\gamma}f,\ \theta(\eta) = \frac{T-T_\infty}{T_w-T_\infty}\ ,\phi(\eta) = \frac{C-C_\infty}{C_w-C_\infty}$$

$$u = \frac{\partial\,\psi}{\partial y} = \frac{\partial\psi}{\partial\eta}\frac{\partial\eta}{\partial y} = xf'(\eta)\sqrt{a\gamma}\sqrt{\frac{a}{\gamma}}\text{ and } v = -\frac{\partial\,\psi}{\partial x} = -f(\eta)\sqrt{a\gamma} \tag{9}$$

From Eq. (4) to Eq. (7)

$$\left(1+\frac{1}{\beta}\right)f''' + Wf''f''' + ff'' - (f')^2 - Mf' - k_pf' - \Delta\theta = 0 \tag{10}$$

$$\frac{1}{Pr}(1+R)\theta'' + Nb\theta'\phi' + Nt(\theta')^2 + f\theta' + Ec\left[\left(1+\frac{1}{\beta}\right)f''^2 + \frac{W}{2}(f'')^3\right] + Q\theta + +Jf'^2 = 0 \tag{11}$$

$$\phi'' + Scf\phi' - ScG\phi + \frac{Nt}{Nb}\theta'' = 0 \tag{12}$$

Boundary conditions:

$$f = 0\ ,\ f' = 1 + \lambda\left[\left(1+\frac{1}{\beta}\right)f'' + \frac{W}{2}(f'')^2\right]\ ,\theta = 1,\ \phi \longrightarrow 1\ as\ \eta \longrightarrow 0$$
$$f'(\eta) = 0, \phi(\eta) \longrightarrow 0, \theta(\eta) \longrightarrow 0\ as\ \eta \longrightarrow \infty \tag{13}$$

The governing parameters are

$$W = \Gamma x\sqrt{\frac{2a^3}{\gamma}}, \lambda = \lambda_1\sqrt{\frac{a}{\gamma}},\ \ \mathrm{M} = \frac{\sigma B_0^2}{a\rho},\ Pr = \frac{\gamma\rho C_p}{\kappa},\ Ec = \frac{(ax)^2}{C_p(T_w-T_\infty)},\ R = \frac{16\sigma^* T_\infty^3}{3k\kappa},$$
$$\Delta = \frac{g\beta'}{a^2x}(T_w - T_\infty),\ k_p = \frac{\gamma}{ak},\quad Nt = \tau\frac{D_T}{\gamma T_\infty}(T_w - T_\infty),\ Nb = \tau\frac{D_B}{\gamma}(C_w - C_\infty), Q = \frac{Q_0}{a\rho C_p},\ Sc = \frac{\gamma}{D_B},$$
$$G = \frac{k_q}{a}\text{ and } J = \frac{\sigma B_0^2}{\rho C_p}\frac{ax^2}{(T_w-T_\infty)}$$

By using Eq. (9) the non-dimensional Cf, Nu_x and Sh_x are expressed as follows

$$Re_x^{\frac{-1}{2}}Cf = -f'(0) = -\left[\left(1+\frac{1}{\beta}\right)f''(0) + \frac{W}{2}\big(f''(0)\big)^2\right]$$

$$Re_x^{\frac{-1}{2}}Nu_x = -\theta'(0) = -(1+R)\theta''(0)$$

$$Re_x^{\frac{-1}{2}}Sh_x = -\phi'(0)$$

3. Method of Solution

We used the most efficient numerical approach in accordance with the R-K method technique to solve the ordinary differential equations (10) to (12) with their related initial and boundary conditions. The numerical solutions are obtained using the symbolic software MATLAB.

$Let\ f = y_{1,} \quad f' = y_2, \quad f'' = y_3$

$\theta = y_4, \quad \theta' = y_5, \quad \phi = y_6, \quad \phi' = y_7$

$\Rightarrow y_1' = y_2, \ y_1(0) = 0, y_2' = y_3$

$y_2(0) = 1 + \lambda\left[\left(1 + \frac{1}{\beta}\right) y_3(0) + \frac{W}{2}\left(y_3(0)\right)^2\right]$

After taking into account the above specified parameters, we arrived at the following results.

$$f''' = y_3' = \frac{(y_2)^2 - y_1 y_3 + (M + k_p) y_2 - \Delta y_4}{\left[\left(1+\frac{1}{\beta}\right) + W y_3\right]}$$

$y_4' = y_5, \quad y_4(0) = 1$

$$\theta'' = \frac{-Pr}{(1+R)}\left\{Nb y_5 y_7 + Nt(y_5)^2 + y_1 y_5 + Ec\left[\left(1 + \frac{1}{\beta}\right) {y_3}^2 + \frac{\mathrm{W}}{2}(y_3)^3\right] + Q y_4 + +J {y_2}^2\right\}$$

$y_6' = y_7, y_6(0) = 1$

$$\phi'' = y_7' = Sc(G y_6 - y_1 y_7) + \frac{Nt}{Nb}\frac{-Pr}{(1+R)}\left\{Nb y_5 y_7 + Nt(y_5)^2 + y_1 y_5 + Ec\left[\left(1 + \frac{1}{\beta}\right) {y_3}^2 + \frac{\mathrm{W}}{2}(y_3)^3\right] + Q y_4 + +J {y_2}^2\right\}$$

To integrate the preceding system of seven first-order simultaneous equations along with their conditions, fourth order RK methodology can be employed. Finally, to meet the convergence condition, the process is repeated until the findings are accurate to the expected level of 10^{-7} accuracy.

4. Result and Discussions

The study investigated the energy, momentum and concentration equations of Casson-Williamson nanofluid flow, which is impacted by the velocity ratio parameter, chemical reaction magnetic field, thermal radiation and Joule heating. We employed the 4th order R-K scheme along the shooting strategy for nonlinear ordinary differential equations (10) to (12) together with the boundary conditions (15). RK methods are known for their high accuracy, especially at moderate step sizes. They can achieve higher-order accuracy (up to 4th, 5th, or even higher) depending on the variant used (e.g., RK4).

Figure 2 velocity and temperature distributions show in Figure 2(a) that when the Casson parameter β declines from 1.0 to 0.0, there is an increase in the velocity of the fluid. In addition, the image in Figure 2(b) illustrates the slight rise in temperature that occurs in reaction to an upsurge in the Casson parameter. Therefore, it can be deduced that the process of rapid cooling necessitates the utilization of no-Newtonian fluid and possesses a Casson parameter that is at its lowest possible value.

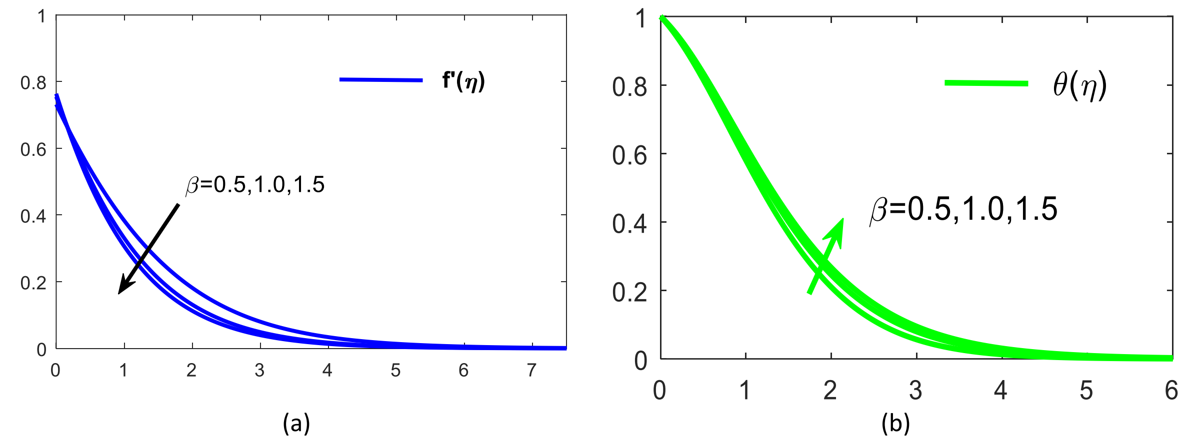

Fig. 2. Casson Parameter (β) v/s (a) f' and (b) θ

Figure 3 depicts the consequences of magnetic field M has on f′, θ and ϕ. The lager values of M nanofluid θ and ϕ rise. However, smaller distributions of velocities are observed, due to the presence of M, the nanofluid motion will be affected by a force that acts as propagation. It will be a physical event. This force has the potential to slow down the nanofluid, decreasing its speed and, eventually, its usefulness. Because of this, some of the heat released by the force that generated the nanofluid is absorbed by it.

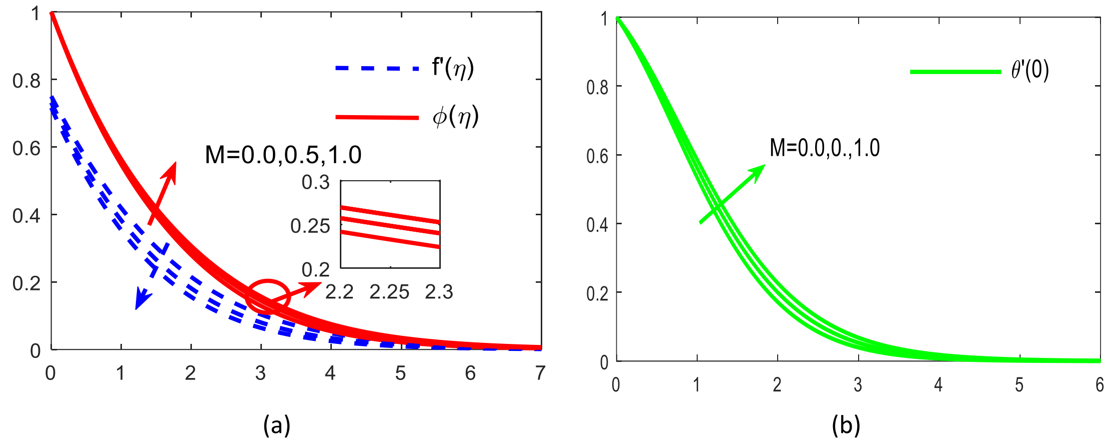

Fig. 3. Magnetic parameter (M) v/s (a) f', ϕ and (b) θ

Figure 4 describes the effects of temperature, nanoparticle concentration, and nanofluid velocity on the mixed convection parameter Δ. The diagram illustrates how the distribution of velocity and thickness of boundary layer improves with the mixed convection parameter; however, the reverse impact is seen when the temperature and concentration profiles decrease. The temperature differential between the sheet and the surrounding air is indicated by the mixed convection parameter in physics. Consequently, a high value for this characteristic indicates, as shown, a weak thermal energy distribution.

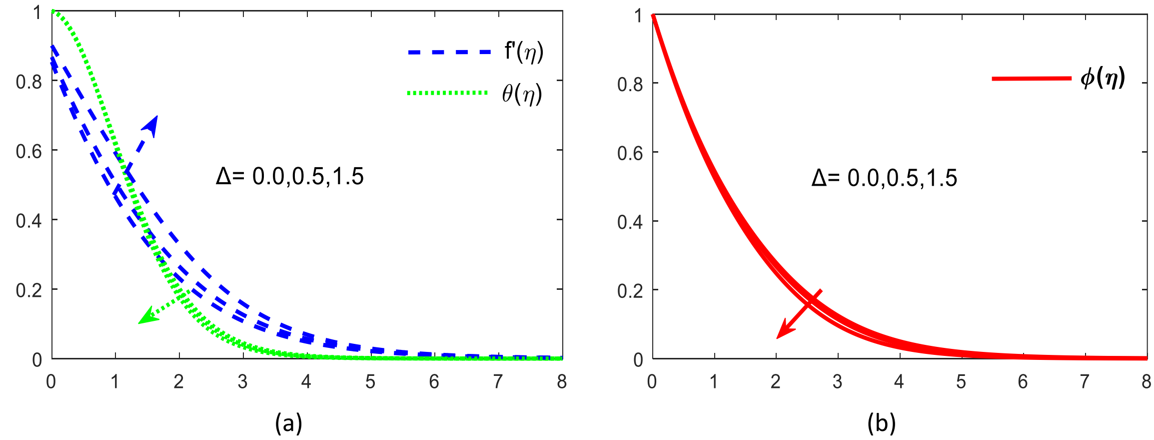

Fig. 4. Mixed convection Parameter v/s (a) f', θ and (b) ϕ

Figure 5 exhibits how the Joule heating parameter J affects the curves of temperature, velocity and concentration. The Joule rule says that the amount of heat made by an electric current is directly related to the temperature of the fluid. Higher values of the Joule heating parameter result in an increase in the temperature of the liquid, indicating a direct correlation between the parameter and the temperature rise. At the same time, the concentration and velocity of the fluid patterns also escape. The interconnection of the porous medium's empty spaces that allow fluid to pass through it is a crucial phenomenon for engineers.

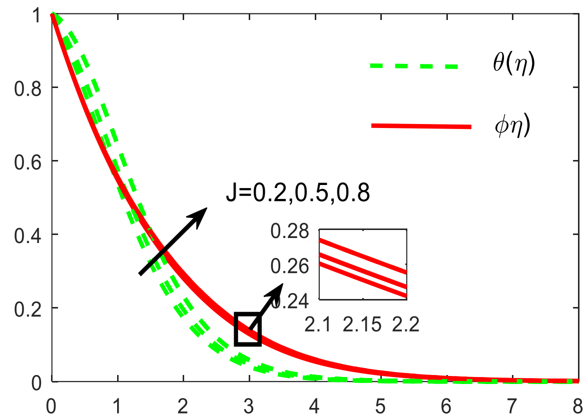

Fig. 5. Joule heating Parameter J v/s f', θ and ϕ

Figure 6 shows that as the porous parameter kp is higher, the velocity profile gets flatter. It was observed that a thinner boundary layer happens for larger values of the viscosity. In addition, shows that altering the porosity parameter also causes temperature fields to arise, increasing the thickness of the thermal boundary layer. As per physics, a high porosity parameter value increases the friction force between liquid layers, which reduces flow velocity and improves temperature distribution.

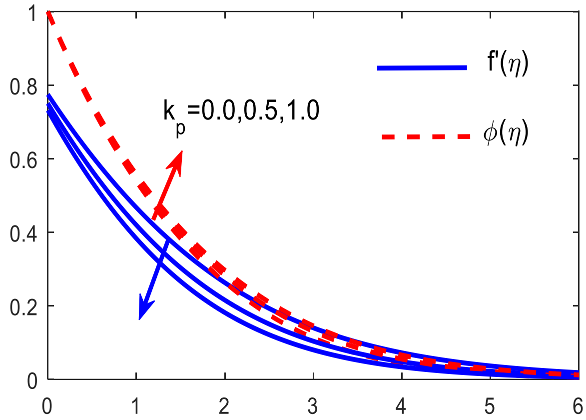

Fig. 6. Porisity parameter Kp v/s f', θ and ϕ

The non-Newtonian nanofluid temperature, velocity and concentration are affected by the slip velocity parameter λ, which is shown in Figure 7. In most cases, when a velocity slip factor is present, it causes a flow-resistive force to operate against the fluid's flow. This force reduces the boundary layer's thickness, which in turn slows the flow of fluid along the sheet. The fluid temperature of the thermal boundary layer is therefore increased. In terms of physical correlation, a high value of slip velocity connected with a rough sheet. So, increased roughness makes fluids more resistant to motion, which slows them down and makes them hotter and more concentrated.

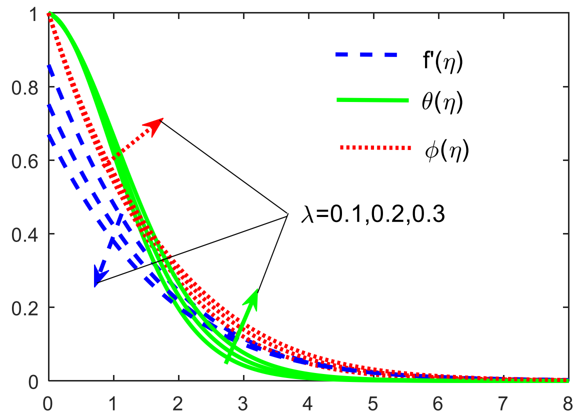

Fig. 7. Slip velocity parameter λ v/s f', θ and ϕ

Figure 8 demonstrates the variation in temperature and nanoparticle concentration using a range of Nb values for Brownian motion. It's interesting to note that while there is reverse trend is seen in temperature, the distribution of concentration is significantly slowed down by the presence of a Brownian parameter. There is a factor here that needs to be considered. A significant motion of nanofluid molecules may occur as a physical consequence of an increase in the Brownian motion parameter. As a result, the kinetic energy is increased, there is an increment in the quantity of heat produced in the boundary layer.

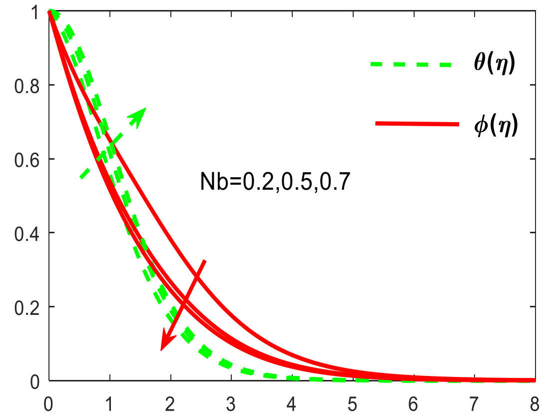

Fig. 8. Nb v/s θ and ϕ

Figure 9 displays the impacts of varying the Eckert number on the temperature and concentration of nanofluid. The Eckert number indicates the conversion of kinetic energy into thermal energy due to friction within the nanofluid. This internal heat generation causes the fluid's temperature to rise and an increase in the thickness of the thermal boundary layer and whereas concentration of Casson –Williamson fluid decreases.

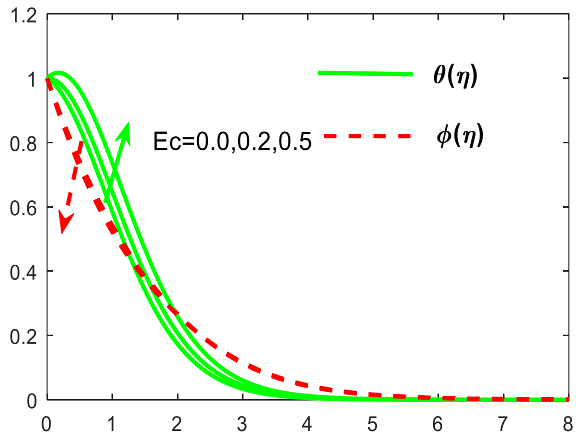

Fig. 9. Eckert number v/s θ and ϕ

The characteristics of the chemical reaction parameter and how it affects the concentration distribution are shown in Figure 10. Increasing the chemical reaction parameter causes the nanofluid concentration to decrease. A decrease in nanofluid concentration brought on by an improved chemical reaction parameter is the cause of this phenomenon, this is essential for optimizing their performance in applications such as heat exchangers, cooling systems.

M = 0.5, beta = 0.5, λ = 0.2, W = 0.5, k = 0.5, A = 0.1, Ec = 0.1, Q = 0.1, J = 0.1, pr = 2.0, Sc = 0.7, Nt = 0.1, Nb = 0.5, R = 0.2, G = 0.2

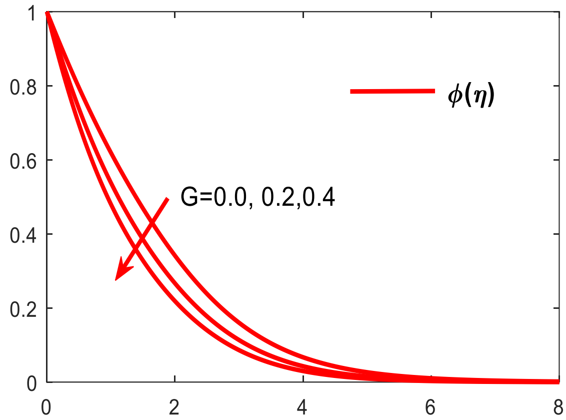

Fig. 10. Chemical reaction v/s Ø

Figure 11 and Figure 12 show the velocity and temperature comparison among the different types fluids. Figure 13 explains Nusselt number is decreasing with the increasing values of $J$and W. Figure 14 it has been discovered that the Skin friction values decline as the value of the magnetic field parameter and porosity values are upsurge. Figure 15 for the higher values of joule heating and velocity parameter heat transfer rate is increasing.

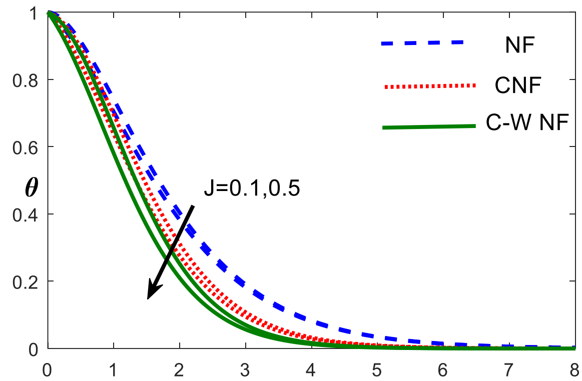

Fig. 11. θ v/s nanofluids

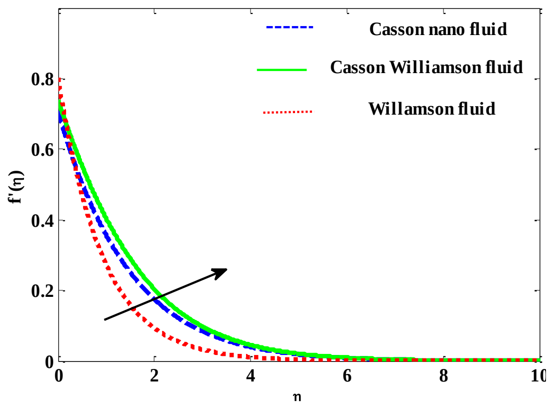

Fig. 12. f′ v/s different types of nanofluids

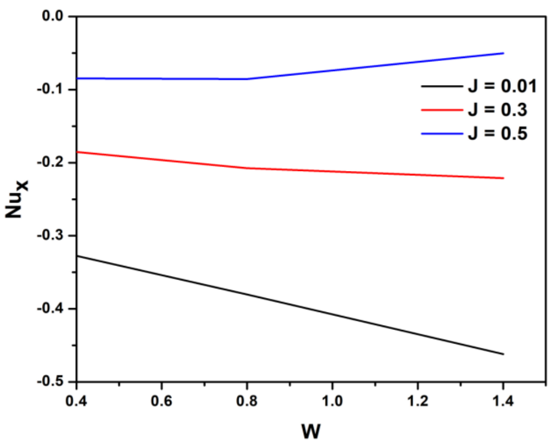

Fig. 13. Nu_x v/s Williamson parameter

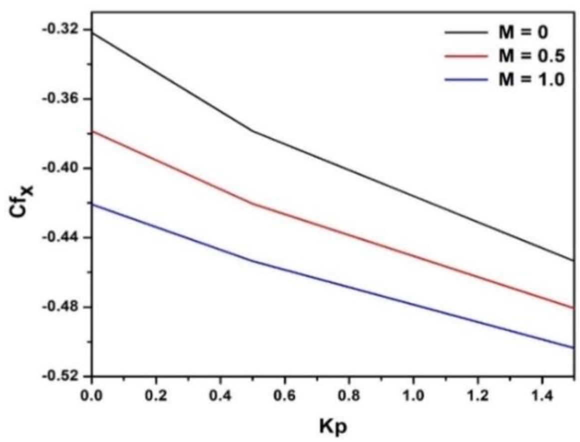

Fig. 14. C_f v/s Porosity parameter

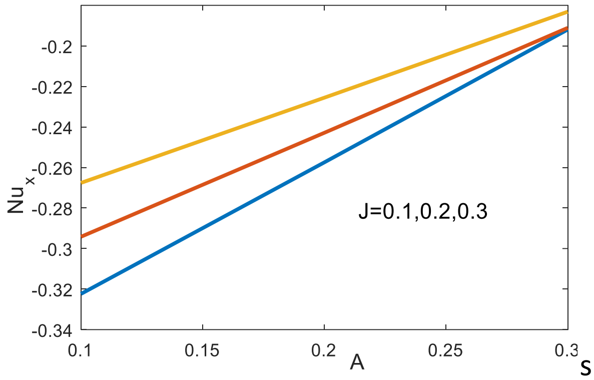

Fig. 15. Nusselt v/s velocity slip parameter

Table 1 shows the interesting fact revealed Skin friction, Heat transfer rate and Sherwood number for various parameters. Table 2 indicates the comparison with the previous results.

Table 1
Numerical values of rate of heat and mass transfer, skin-friction coefficient for variation of $M, k_p, R, Ec, Sc, W, J, \beta, Nb, Le, \lambda, Bi, Cf, Nu_x$ and Sh_x

M	k_p	R	Nb	Ec	J	Sc	β	W	$-Cf$	$-Nu_x$	$-Sh_x$
0.0									0.365055	0.375061	0.582407
0.5									0.402850	0.339951	0.569257
1.0									0.432169	0.309574	0.559429
	0.0								0.365055	0.375061	0.582407
	0.5								0.402850	0.339951	0.569257
	1.5								0.455904	0.282405	0.551871
		1.0							0.400038	0.289605	0.575250
		3.0							0.395306	0.205199	0.586455
		5.0							0.392382	0.159268	0.592639
			0.2						0.403994	0.459021	0.487514
			0.5						0.402850	0.339951	0.569257
			0.7						0.402084	0.271466	0.583612
				0.0					0.403376	0.392852	0.559996
				0.2					0.402325	0.287275	0.578475
				0.3					0.401802	0.234822	0.587650
					0.01				0.402850	0.339951	0.569257
					0.3				0.401553	0.191102	0.562145
					0.5				0.400638	0.086067	0.557404
						4.0			0.402968	0.255538	1.547537
						6.0			0.403158	0.246597	1.917385
						8.0			0.403301	0.241977	2.227839
							0.5		0.402850	0.339951	0.569257
							1.5		0.598279	0.303481	0.551796
							2.5		0.668529	0.295805	0.546480s
								0.0	0.485769	0.283857	0.552852
								0.4	0.420481	0.327586	0.565262
								0.8	0.346772	0.380355	0.583854

Table 2
Comparison of $-f'(0)$ values when $k_p = \Delta = \lambda = W = 0\ and\ \beta \longrightarrow \infty$

M	Present Values $(-C_f)$	Mahmoud
0.0	1.00000	1.00140
1.0	1.414214	1.41424
3.0	2.0000	2.00000
5.0	2.449490	2.44950

5. Conclusions

The combined effect of slip velocity and joule heating phenomena is a novel approach utilized to represent the flow of a non-Newtonian CWN owing to a stretched sheet. Heat generation (absorption), thermal radiation, magnetic fields, and chemical reactions between nanoparticles are also considered. Moreover, a porous saturated material surrounds the physical model. The shooting method is used to graphically represent the numerical study, which is covered in full. We will now discuss the results in further detail

i. The higher values of Joule heating J suppresses θ(η) which in turn causes the enhancement of Nu_x.
ii. The temperature profiles drop as mixed convection parameter rises, while it increases with the higher values of magnetic, joule heating and Brownian motion parameters.
iii. The joule heating raises the temperature and concentration of the Fluid, while Williamson parameter is affects in the opposite direction.
iv. The higher values of magnetic field enhance the temperature and concentration
v. It is intriguing to note that the effect porous medium k_p is so influencing and depreciates the velocity field.

This study paves the way for future research on the influence on heat and mass transmission of MHD nanofluid flow with the velocity slip, joule heating, and the Chemical reaction effects. The same combined effects of the factors in this study can be analysed using another type of Nano fluids.

Applications
The process is essential in cooling and refrigeration (instant cold packs), food preparation (cooking), biological processes (sweating), and industrial applications.

Conflict of interest
The authors declare no conflict of interest.

Funding
This research received no external funding.

Author contributions
While R.K. came up with the concept for the study and investigated potential implementations in software, B.S.R. and Y.N. carried out the analysis and wrote the paper. Responsible for conceptualization and methodology are R.K. and B.S.R.; validation, formal analysis, and investigation are R.K., B.S.R., and Y.N.; resources, data curation, and writing (original draft preparation, review, and editing) are R.K. and B.S.R.; and supervision, project administration, and funding acquisition by R.K. and D.H. All authors have read and agreed to the published version of the manuscript.

References

[1] Choi, S. U. S., Z. G. Zhang, W. Yu, F. E. Lockwood, and E. A. Grulke. "Anomalous thermal conductivity enhancement in nanotube suspensions." *Applied Physics Letters* 79, no. 14 (2001): 2252-2254. https://doi.org/10.1063/1.1408272

[2] Nima, Nayema Islam, S. O. Salawu, M. Ferdows, M. D. Shamshuddin, Abdulaziz Alsenafi, and A. Nakayama. "Melting effect on non-Newtonian fluid flow in gyrotactic microorganism saturated non-darcy porous media with variable fluid properties." *Applied Nanoscience* 10 (2020): 3911-3924. https://doi.org/10.1007/s13204-020-01491-y

[3] El-Khatib, Ahmed M., N. S. Yousef, Z. F. Ghatass, Mohamed S. Badawi, M. M. Mohamed, and Mostafa Elkhatib. "Synthesized silver carbon nanotubes and zinc oxide nanoparticles and their ability to remove methylene blue dye." *Journal of Nano Research* 56 (2019): 1-16. https://doi.org/10.4028/www.scientific.net/JNanoR.56.1

[4] El-khatib, Ahmed M., M. Elsafi, M. I. Sayyed, M. I. Abbas, and Mostafa El-Khatib. "Impact of micro and nano aluminium on the efficiency of photon detectors." *Results in Physics* 30 (2021): 104908. https://doi.org/10.1016/j.rinp.2021.104908

[5] Khalil, Alaa Mahmoud, Ahmed Mohamed El-Khatib, and Mostafa El-khatib. "Synthesis of hexagonal nanozinc by arc discharge for antibacterial water treatment." *Surface Innovations* 8, no. 3 (2019): 165-171. https://doi.org/10.1680/jsuin.19.00050

[6] Buongiorno, Jacopo. "Convective transport in nanofluids." *ASME Journal of Heat and Mass Transfer* 128, no. 3 (2006): 240-250. https://doi.org/10.1115/1.2150834

[7] Kumar, Amit, Ramayan Singh, Gauri Shanker Seth, and Rajat Tripathi. "Soret effect on transient magnetohydrodynamic nanofluid flow past a vertical plate through a porous medium with second order chemical reaction and thermal radiation." *International Journal of Heat and Technology* 36, no. 4 (2018): 1430-1437. https://doi.org/10.18280/ijht.360435

[8] Kumar, B., G. S. Seth, and R. Nandkeolyar. "Quadratic multiple regression model and spectral relaxation approach to analyse stagnation point nanofluid flow with second-order slip." *Proceedings of the Institution of Mechanical Engineers, Part E: Journal of Process Mechanical Engineering* 234, no. 1 (2020): 3-14. https://doi.org/10.1177/0954408919878984

[9] Patel, Harshad R., Akhil S. Mittal, and Rakesh R. Darji. "MHD flow of micropolar nanofluid over a stretching/shrinking sheet considering radiation." *International Communications in Heat and Mass Transfer* 108 (2019): 104322. https://doi.org/10.1016/j.icheatmasstransfer.2019.104322

[10] Saeed, Syed Tauseef, Muhammad Bilal Riaz, Jan Awrejcewicz, and Hijaz Ahmad. "Exact symmetric solutions of MHD Casson fluid using chemically reactive flow with generalized boundary conditions." *Energies* 14, no. 19 (2021): 6243. https://doi.org/10.3390/en14196243

[11] Qayyum, Mubashir, Tariq Abbas, Sidra Afzal, Syed Tauseef Saeed, Ali Akgül, Mustafa Inc, Khaled H. Mahmoud, and Abdullah Saad Alsubaie. "Heat transfer analysis of unsteady MHD Carreau fluid flow over a stretching/shrinking sheet." *Coatings* 12, no. 11 (2022): 1661. https://doi.org/10.3390/coatings12111661

[12] Firdous, Hina, Syed Tauseef Saeed, Hijaz Ahmad, and Sameh Askar. "Using non-Fourier's heat flux and non-Fick's mass flux theory in the radiative and chemically reactive flow of Powell-Eyring fluid." *Energies* 14, no. 21 (2021): 6882. https://doi.org/10.3390/en14216882

[13] Megaraju, P., Siva Reddy Sheri, and Raja Shekar. "Transient MHD flows through an exponentially accelerated isothermal vertical plate with Hall effect and chemical reaction effect: FEM." *Partial Differential Equations in Applied Mathematics* 4 (2021): 100047. https://doi.org/10.1016/j.padiff.2021.100047

[14] Nima, Nayema Islam, S. O. Salawu, M. Ferdows, M. D. Shamshuddin, Abdulaziz Alsenafi, and A. Nakayama. "Melting effect on non-Newtonian fluid flow in gyrotactic microorganism saturated non-darcy porous media with variable fluid properties." *Applied Nanoscience* 10 (2020): 3911-3924. https://doi.org/10.1007/s13204-020-01491-y

[15] Chinyoka, T., and O. D. Makinde. "Computational dynamics of unsteady flow of a variable viscosity reactive fluid in a porous pipe." *Mechanics Research Communications* 37, no. 3 (2010): 347-353. https://doi.org/10.1016/j.mechrescom.2010.02.007

[16] Rajput, Govind R., M. D. Shamshuddin, and Sulyman O. Salawu. "Thermosolutal convective non-Newtonian radiative Casson fluid transport over a vertical plate propagated by Arrhenius kinetics with heat source/sink." *Heat Transfer* 50, no. 3 (2021): 2829-2848. https://doi.org/10.1002/htj.22008

[17] Raza, Jawad, Azizah Mohd Rohni, and Zurni Omar. "Multiple solutions of mixed convective MHD Casson fluid flow in a channel." *Journal of Applied Mathematics* 2016, no. 1 (2016): 7535793. https://doi.org/10.1155/2016/7535793

[18] Qing, Jia, Muhammad Mubashir Bhatti, Munawwar Ali Abbas, Mohammad Mehdi Rashidi, and Mohamed El-Sayed Ali. "Entropy generation on MHD Casson nanofluid flow over a porous stretching/shrinking surface." *Entropy* 18, no. 4 (2016): 123. https://doi.org/10.3390/e18040123

[19] Khan, Muhammad Ijaz, Muhammad Waqas, Tasawar Hayat, and Ahmed Alsaedi. "A comparative study of Casson fluid with homogeneous-heterogeneous reactions." *Journal of Colloid and Interface Science* 498 (2017): 85-90. https://doi.org/10.1016/j.jcis.2017.03.024

[20] Khan, Najeeb Alam, Sidra Khan, and Fatima Riaz. "Boundary layer flow of Williamson fluid with chemically reactive species using scaling transformation and homotopy analysis method." *Mathematical Sciences Letters* 3, no. 3 (2014): 199. https://doi.org/10.12785/msl/030311

[21] Khan, Masood, and Aamir Hamid. "Numerical investigation on time-dependent flow of Williamson nanofluid along with heat and mass transfer characteristics past a wedge geometry." *International Journal of Heat and Mass Transfer* 118 (2018): 480-491. https://doi.org/10.1016/j.ijheatmasstransfer.2017.10.126

[22] Shamshuddin, M. D., F. Mabood, and S. O. Salawu. "Flow of three-dimensional radiative Williamson fluid over an inclined stretching sheet with Hall current and nth-order chemical reaction." *Heat Transfer* 50, no. 6 (2021): 5400-5417. https://doi.org/10.1002/htj.22130

[23] Subbarayudu, K., S. Suneetha, and P. Bala Anki Reddy. "The assessment of time dependent flow of Williamson fluid with radiative blood flow against a wedge." *Propulsion and Power Research* 9, no. 1 (2020): 87-99. https://doi.org/10.1016/j.jppr.2019.07.001

[24] Mishra, Ashish. "Thompson and Troian slip effects on ternary hybrid nanofluid flow over a permeable plate with chemical reaction." *Numerical Heat Transfer, Part B: Fundamentals* (2024): 1-29. https://doi.org/10.1080/10407790.2024.2346929

[25] Khan, M., M. Azam, and A. S. Alshomrani. "Unsteady slip flow of Carreau nanofluid over a wedge with nonlinear radiation and new mass flux condition." *Results in Physics* 7 (2017): 2261-2270. https://doi.org/10.1016/j.rinp.2017.06.038

[26] Humane, Pooja P., Vishwambhar S. Patil, and Amar B. Patil. "Chemical reaction and thermal radiation effects on magnetohydrodynamics flow of Casson-Williamson nanofluid over a porous stretching surface." *Proceedings of the Institution of Mechanical Engineers, Part E: Journal of Process Mechanical Engineering* 235, no. 6 (2021): 2008-2018. https://doi.org/10.1177/09544089211025376

[27] Reddy, Y. Dharmendar, V. Srinivasa Rao, D. Ramya, and L. Anand Babu. "MHD boundary layer flow of nanofluid and heat transfer over a nonlinear stretching sheet with chemical reaction and suction/blowing." *Journal of Nanofluids* 7, no. 2 (2018): 404-412. https://doi.org/10.1166/jon.2018.1450

[28] Swarnalathamma, B. V., DM Praveen Babu, and M. Veera Krishna. "Combined impacts of radiation absorption and chemically reacting on MHD free convective Casson fluid flow past an infinite vertical inclined porous plate." *Journal of Computational Mathematics and Data Science* 5 (2022): 100069. https://doi.org/10.1016/j.jcmds.2022.100069

[29] Yousef, N. S., Ahmed M. Megahed, Nourhan I. Ghoneim, M. Elsafi, and Eman Fares. "Chemical reaction impact on MHD dissipative Casson-Williamson nanofluid flow over a slippery stretching sheet through porous medium." *Alexandria Engineering Journal* 61, no. 12 (2022): 10161-10170. https://doi.org/10.1016/j.aej.2022.03.032

[30] Goud, B. Shankar, Y. Dharmendar Reddy, and V. Srinivasa Rao. "Thermal radiation and Joule heating effects on a magnetohydrodynamic Casson nanofluid flow in the presence of chemical reaction through a non-linear inclined porous stretching sheet." *Journal of Naval Architecture and Marine Engineering* 17, no. 2 (2020): 143-164. https://doi.org/10.3329/jname.v17i2.49978

[31] Nadeem, S., and S. T. Hussain. "Heat transfer analysis of Williamson fluid over exponentially stretching surface." *Applied Mathematics and Mechanics* 35, no. 4 (2014): 489-502. https://doi.org/10.1007/s10483-014-1807-6